

Differentiated Relevances Embedding for Group-based Referring Expression Comprehension

Fuhai Chen, *Student Member, IEEE*, Xiaoshuai Sun*, *Member, IEEE*, Xuri Ge, Jianzhuang Liu, *Member, IEEE*, Yongjian Wu, *Member, IEEE*, Feiyue Huang, *Member, IEEE*, and Rongrong Ji, *Senior Member, IEEE*,

arXiv:2203.06382v1 [cs.CV] 12 Mar 2022

Abstract—Referring expression comprehension (REC) aims to locate a certain object in an image referred by a natural language expression. For joint understanding of regions and expressions, existing REC works typically target on modeling the cross-modal relevance in each region-expression pair within each single image. In this paper, we explore a new but general REC-related problem, named Group-based REC, where the regions and expressions can come from different subject-related images (images in the same group), e.g., sets of photo albums or video frames. Different from REC, Group-based REC involves differentiated cross-modal relevances within each group and across different groups, which, however, are neglected in the existing one-line paradigm. To this end, we propose a novel relevance-guided multi-group self-paced learning schema (termed RMSL), where the within-group region-expression pairs are adaptively assigned with different priorities according to their cross-modal relevances, and the bias of the group priority is balanced via an across-group relevance constraint simultaneously. In particular, based on the visual and textual semantic features, RMSL conducts an adaptive learning cycle upon triplet ranking, where (1) the target-negative region-expression pairs with low within-group relevances are used preferentially in model training to distinguish the primary semantics of the target objects, and (2) an across-group relevance regularization is integrated into model training to balance the bias of group priority. The relevances, the pairs, and the model parameters are alternatively updated upon a unified self-paced hinge loss. Quantitative experiments on three widely-used REC benchmarks (RefCOCO, RefCOCO+, and RefCOCOg) demonstrate the superiority of the proposed RMSL method against the state-of-the-art methods. Extensive ablative experiments are conducted to further demonstrate the effectiveness of RMSL on modeling differentiated within-group and across-group relevances.

Index Terms—Referring expression comprehension (REC), group-based, differentiated relevance, adaptive learning.

I. INTRODUCTION

REFERRING expression comprehension (REC) aims to locate a particular object in an image referred by a given natural language expression, such as locating *a lady in an olive shirt* among all the persons as illustrated in Fig. 1. The challenge of REC lies in joint understanding of

F. Chen, X. Sun, and X. Ge are with the Media Analytics and Computing Lab, Department of Artificial Intelligence, School of Informatics, Xiamen University, 361005, China. X. Sun is the corresponding author of this paper (Email: xssun@xmu.edu.cn).

R. Ji is with the Media Analytics and Computing Lab, Department of Artificial Intelligence, School of Informatics, Xiamen University, 361005, China, and Peng Cheng Laboratory, Shenzhen, 518055, China (e-mail: rrji@xmu.edu.cn).

J. Liu is with the Huawei Noahs Ark Lab, Shenzhen, China.

Y. Wu and F. Huang are with Tencent YouTu Lab, Shanghai, China.

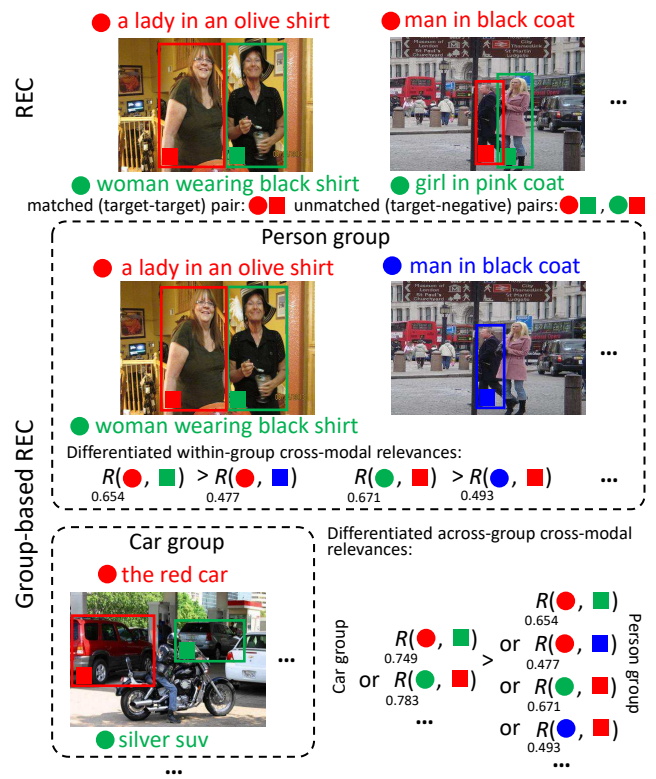


Fig. 1. Top: traditional referring expression comprehension (REC), where the matched/unmatched region-expression pairs are constructed from each image (the targets are illustrated in red). Typically, the cross-modal relevance of each matched/unmatched pair is maximized/minimized for REC model training. Middle and Bottom: Group-based REC, where the cross-modal relevances of the unmatched pairs are differentiated within each group and across different groups.

visual and textual domains, where the target-negative cross-modal relevances (matching scores) need to be measured to distinguish the target regions/expressions and the negative regions/expressions as shown in Fig. 1. To this end, existing REC works [1]–[5] typically adopt a ranking-based triplet hinge loss to maximize the matching score of each matched (target-target) region-expression pair while minimize the unmatched (target-negative) ones in each image. This leads the models to learn to extract the discriminative features of the regions and expressions for their correct alignments. However, these works focus on model training under a one-line paradigm, leaving the region-expression alignments from multiple images unexplored. In contrast, in many applications like grounding expressions on multiple surveillance frames and screens, objects are expected to be located among multiple

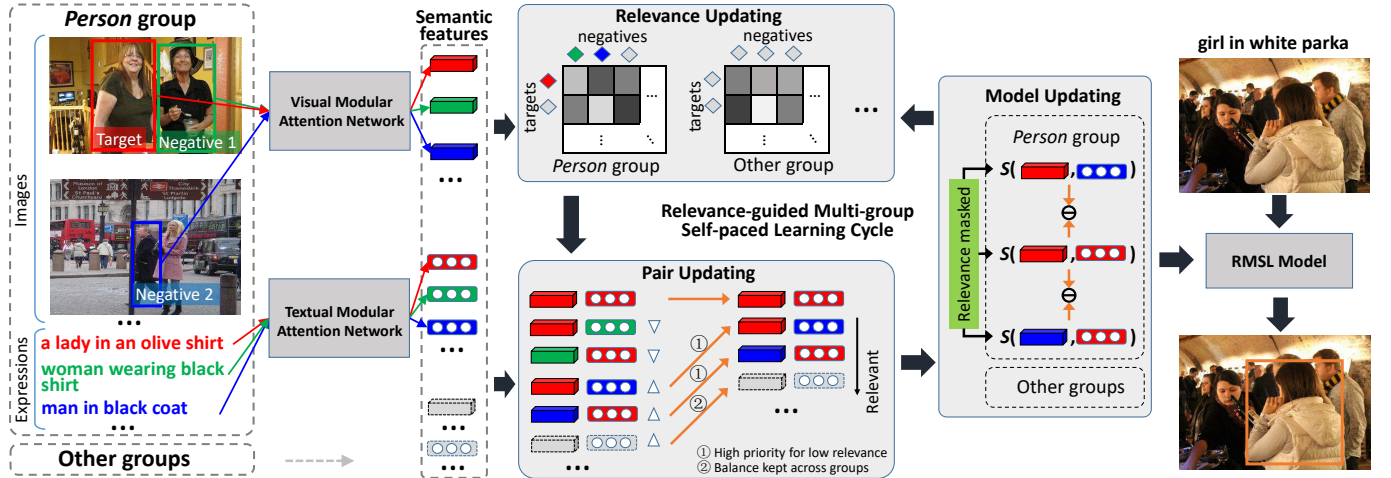


Fig. 2. The framework of the proposed relevance-guided multi-group self-paced learning schema (RMSL) for Group-based REC. It consists of three main components, *i.e.*, *Relevance Updating*, *Pair Updating*, and *Model Updating*. In particular, given the grouped images and expressions, RMSL (1) initializes/updates the semantic features of the pairs and the within-group cross-modal relevances in *Relevance Updating*, where the semantic features of the object regions and expressions are extracted using visual and textual modular attention networks following [1], [2], respectively, (2) assigns the unmatched pairs with different priorities according to their within-group cross-modal relevances and selects those with low relevances in *Pair Updating*, and (3) minimizes a relevance-masked triplet hinge loss based on the matching scores of the matched/unmatched pairs under the across-group relevance constraint during *Model Updating*. Steps (1)~(3) proceed in each training iteration, where the relevances, the pairs, and the model parameters are alternatively updated in a unified and adaptive end-to-end manner. During localization, given an image and an expression query, the pseudo object is localized by utilizing the trained model.

subject-related images (group). This inspires us to explore a new problem, named Group-based Referring Expression Comprehension (termed *Group-based REC*), which can be defined as learning an expression-to-region model among groups to locate the unique object referred by a given natural language expression as shown in Fig. 1.

Different from REC, Group-based REC involves the differentiated within-group and differentiated across-group cross-modal relevances in REC model training. On one hand, the cross-modal relevances vary a lot within each group. For example, in Fig. 1, *a lady in an olive shirt* vs. *man in black coat* is less relevant than *a lady in an olive shirt* vs. *woman wearing black shirt* according to the gender and the type of the clothes. In order to enable the model to distinguish the primary semantics such as *shirt* vs. *coat* and *male* vs. *female*, the pair of *a lady in an olive shirt* vs. *man in black coat* should be naturally learned with higher priority than the pair of *a lady in an olive shirt* vs. *woman wearing black shirt*. This is also revealed in [6]–[8], which declare that the model should be trained by using the diverse data dynamically. These lead to a potential solution of embedding the within-group cross-modal relevances dynamically into the REC model learning, for instance, by assigning the lowly relevant unmatched pair with higher priority within each group in the early training iterations. On the other hand, there exists a large variety of the cross-modal relevances across different groups. For example, in Fig. 1, the overall relevance of the *Car* group is apparently larger than that of the *Person* group due to the subtle and non-rigid variations of the latter one. This is also reflected by Coefficient of Variation¹ 15.64% over different groups, calculated based on the results of the REC state-of-the-art method [2]

on the standard dataset, RefCOCOg [3]. Thus, simply using the unmatched training pairs for model training upon their differentiated cross-modal relevances would probably lead the model to overfitting to certain groups.

In this paper, we aim to address two essential issues for Group-based REC, *i.e.* the embedding of the differentiated within-group and across-group cross-modal relevances. Our first goal is to assign the within-group unmatched pairs with different priorities dynamically according to their cross-modal relevances in an adaptive model training, where the unmatched pairs with low relevances should be prior to the ones with high relevances. Our second goal is to enforce a balanced training to reduce the bias of the training priority derived from the inherent relevance variance of different groups. This encourages various unmatched pairs from different groups to be considered during the adaptive model training.

Driven by the above insights, we propose a novel relevance-guided multi-group self-paced learning method (termed RMSL) to embed the differentiated within-group and across-group cross-modal relevances for Group-based REC. Our main innovations lie in two aspects. Firstly, inspired by self-paced learning [10]–[12] where the model is learned by gradually using samples from easy to complex according to their losses, we introduce a relevance-guided adaptive learning strategy to embed the differentiated within-group cross-modal relevances for REC model training, where the within-group unmatched pairs are automatically assigned with different priorities along with their cross-modal relevances updated. Secondly, to enforce a balanced training, we integrate an across-group cross-modal relevance constraint over the unmatched pairs of different groups into the adaptive REC model training, where the across-group variety of the unmatched pairs is formulated via a relevance-based regularization term.

In particular, as illustrated in Fig. 2, given the grouped

¹Coefficient of Variation (CV) [9] represents the ratio of the standard deviation to the mean, which is a statistical measure of the dispersion of data points in a data series around the mean.

unmatched pairs², where the semantic features of the object regions and expressions are initially extracted based on Faster-RCNN [13] and Bi-directional LSTM (Bi-LSTM) [14] following [1], [2], respectively, RMSL is trained adaptively via a relevance-guided multi-group self-paced learning cycle: (1) The visual and textual semantic features of pairs are used to update/initialize their within-group cross-modal relevances in *Relevance Updating*. (2) The pairs are assigned with different priorities and selected subsequently in *Pair Updating* according to their within-group cross-modal relevances. (3) To distinguish the target and negative regions/expressions among the groups, a relevance-masked triplet hinge loss are minimized based on the matching scores of the matched/unmatched pairs during *Model Updating*, where an across-group relevance-based regularization term is maximized to reduce the group-wise relevance sparsity. Thus, the parameters of feature extraction and matching operation are optimized in this stage. New semantic features of the pairs derived from this temporarily optimized model are used to update the within-group cross-modal relevances in the step (1). We cycle steps (1)~(3) in different iterations to adjust priorities of the pairs adaptively, where the relevances, the pairs, and the model parameters are alternatively updated in a unified end-to-end manner. During the localization, given an image and an expression query, the pseudo object can be localized based on the optimized model. We conduct quantitative experiments on three widely-used REC benchmarks (RefCOCO, RefCOCO+, and RefCOCOg), which demonstrate the superiority of the proposed RMSL method against the state-of-the-art methods [1], [2], [5], [15]–[17]. Extensive ablative experiments are also conducted to further demonstrate the effectiveness of RMSL on modeling differentiated within-group and across-group relevances.

In summary, the paper makes the following contributions: (1) We investigate a new problem, termed Group-based referring expression comprehension (Group-based REC). (2) We are the first to consider the differentiated within-group and across-group cross-modal relevances of the region-expression pairs. (3) A novel adaptive learning strategy, *i.e.*, relevance-guided multi-group self-paced learning strategy (RMSL), is proposed to model the within-group and across-group cross-modal relevances for Group-based REC. (4) The proposed RMSL method achieves state-of-the-art in three commonly-used REC benchmarks.

The rest of paper is organized as follows: Section II reviews the related work. In Section III, we introduce the proposed relevance-guided multi-group self-paced learning method (RMSL) for Group-based REC. Experimental evaluations and comparisons are given in Section IV. And finally, we conclude this paper in Section V.

II. RELATED WORK

Referring Expression Comprehension (REC). The task of REC is to localize a special object referred by a given expression query in an image. To address this problem, recent

²We group the unmatched region-expression pairs according to their subjective categories in the expressions. The category list has been predefined in the REC datasets, *e.g.*, *Person* category. Details are provided in the Section III-B.

methods [1]–[3], [16] widely adopt the ranking-based learning schema with the region-expression pairs in each individual image. Specially, some [3], [4], [15], [18], [19] use the trained generation model (such as CNN-RNN) to model the expression probability given the object region and look for a region that leads to a maximal expression probability. Others [1], [2], [5], [20], [21] learn a joint embedding space for the object regions and the expressions by maximizing the relevance of matched region-expression pairs and minimizing the unmatched ones. In this learning way, they aim to find the region with maximal probability given the expression directly. In practice, the latter performs better as summarized in [5], which is probably due to more discriminative representation of object regions and expressions in the max-margin pattern. Among them, the works [1], [2] propose the modular attention networks to parse and represent the semantic contents in both visual and textual channels. For example, [2] design a Faster-RCNN based visual and a Bi-LSTM based textual modular attention networks to extract the semantic features of the subjects, locations, and relationships in the images and the expressions. And it achieves current state-of-the-art performances due to its rich semantic representation.

Different from the methods above, this paper explores a new problem, *i.e.*, Group-based REC, which involves the differentiated within-group and the differentiated across-group cross-modal relevances of the region-expression pairs. Accordingly, the proposed RMSL doesn't innovate in the feature representation but the adaptive learning strategy. To ensure the fairness on the evaluations, we keep the same number of the training samples and the same batch size of region-expression pairs for model training. Detailed experiments and analysis are provided in Section IV.

Self Paced Learning. Inspired by the learning process of humans and animals, Curriculum Learning (CL) [22]–[26] and Self-paced Learning (SPL) [10], [27]–[29] have been extensively investigated in these years. The idea is to learn the model iteratively from easy samples to hard samples. These two methods share a similar conceptual learning paradigm, but differ in specific learning schemes. In CL, the curriculum is predetermined by prior knowledge, and remain fixed thereafter. Therefore, this type of method heavily relies on the quality of prior knowledge while ignoring feedback about the learner. On the contrary, the curriculum of SPL is dynamically determined to adjust to the learning pace of the leaner. And SPL has been proved to be more effective in many tasks due to its generality and adaptivity, such as object/saliency detection [30]–[32], person re-identification [33], [34], image classification [12], [35], [36], and multimedia event detection [7], [11], [37].

Most of the previous works only consider sample easiness for sampling in SPL, where the loss of the sample in each training iteration is taken as the estimation of its easiness. Although Jiang *et al.* [7] and Zhang *et al.* [31] make the efforts to additionally integrate sample diversity in SPL, the sample diversity is estimated according to the diversity of the sample loss, which also depends on the sample easiness. These traditional loss-guided SPL methods are infeasible in Group-based REC because: (1) REC is inherently set to avoid distinguishing the easy and the hard samples [3], (2) the core

factor of REC is cross-modal relevance [1], [2], which is naturally taken as the guidance of the training rather than the sample loss, and (3) the characteristic of Group-based REC is differentiated cross-modal relevance derived from the internal multi-modal semantic contents, which is different from the loss-based sample diversity or the loss-based group diversity.

III. RMSL FOR GROUP-BASED REC

In this section, we first describe the problem formulation of REC and the proposed Group-based REC in Section III-A. Next, we introduce the proposed relevance-guided multi-group self-paced learning scheme (RMSL). For readability, we separate the adaptive priority assignment, including relevance updating and pair updating, from the holistic schema in Section III-B. Finally, we formulate RMSL objective and describe its optimizing strategy in Section III-C.

A. Problem Formulation

Referring expression comprehension (REC) aims to locate a particular object in an image referred by a given natural language expression, which is typically set as a ranking-based retrieval problem: given an image, a query expression (sentence), and a set of object region proposals extracted from the image, the proposal with the highest matching score is chosen as the target object according to the matching score between each region proposal and the query. For the model training, suppose there are N matched region-expression pairs, a ranking-based triplet hinge loss can be formulated based on the region proposals $\{v_i | i \in 1, \dots, N\}$ and the expressions $\{s_i | i \in 1, \dots, N\}$:

$$\begin{aligned} \min_{\theta} \sum_{i=1}^N & \left[\max(0, \Delta + F(v_i, s_j; \theta) - F(v_i, s_i; \theta)) \right. \\ & \left. + \max(0, \Delta + F(v_k, s_i; \theta) - F(v_i, s_i; \theta)) \right], \quad (1) \\ & \text{s.t. } i \neq j \text{ and } i \neq k, \end{aligned}$$

where s_j and v_k are randomly sampled from the same image as v_i and s_i . Δ denotes the margin of the hinge loss. $F(v, s; \theta)$ returns a matching score of v and s by extracting their semantic features and feeding them to an MLP (multi-layer perception) layer and an L2 normalization layer as set in [2]. θ is the parameter set of the feature extraction and the matching operation. In the max-margin pattern, F outputs a high matching score for the matched region-expression pair $\langle v_i, s_i \rangle$, while it outputs low matching scores for the unmatched region-expression pairs $\langle v_i, s_j \rangle$ and $\langle v_k, s_i \rangle$.

In Group-based REC, the region v_i and the expression s_j (or v_k and s_i) of the unmatched pair can come from different images but within a same group.³ The goal of Group-based REC is to learn a REC model upon the grouped region-expression pairs to locate the correct object referred by a given expression. Suppose there are N_G groups of the matched region-expression pairs, $\{\mathcal{G}_g | g = 1, \dots, N_G\}$, these pairs can

³Since the variety of the unmatched pairs may contribute to the gain of the REC performance, but it has been verified that the randomly sampling way is still trapped in the effect of the differentiated within-group and across-group relevances in Section IV.

TABLE I
MAIN NOTATIONS AND THEIR DEFINITIONS (EXCLUDING THE ONES OF FEATURE EXTRACTION)

Notation	Definition
N	the number of the matched region-expression pairs
N_G	the number of groups
\mathcal{G}_g	the set of the matched region-expression pairs in the g -th group
N_g	the number of the matched region-expression pairs in \mathcal{G}_g
M	the number of the matched region-expression pairs (targets) in a batch
M'	the number of the negatives in a batch
s	the expression
v	the region proposal
$\langle v, s \rangle$	a region-expression pair
$\mathbf{s} \in R^{3d}$	the feature vector of the expression
$\mathbf{v} \in R^{3d}$	the feature vector of the region proposal
\mathcal{P}	a matched pair set with M pairs in a certain batch
$\mathcal{P}'_1, \mathcal{P}'_2$	two unmatched pair sets for the target-negative and negative-target pairs respectively in a certain batch
$\mathbf{R}^{(g)} \in R^{M \times M'}$	the relevance matrix of the g -th group
$\mathbf{U}^{(g)} \in R^{M \times M'}$	a binary priority matrix of the g -th group
$\mathcal{U} = \{\mathbf{U}^{(g)}\}_{g=1}^{N_G}$	the set/combination of the binary priority matrices over N_G groups
θ	the parameter set of the feature extraction and matching operation
Δ	the margin of the hinge loss
$\alpha \in \{0, 1\}$	a switch coefficient to choose the visual or textual features for the relevance estimation
λ_1, λ_2	the adaptive parameters to control the learning pace for the visual and textual relevances, respectively
γ	the dynamically-changing coefficient of the across-group relevance regularization
τ	a fixed trade-off coefficient of the relevance threshold
μ_1, μ_2	the updating coefficients of λ_1 and λ_2 , respectively
η	the rising rate of γ

be represented as $\{\langle v_i^{(g)}, s_i^{(g)} \rangle | v_i^{(g)}, s_i^{(g)} \in \mathcal{G}_g\}_{g=1}^{N_G}$ ⁴ where the g -th group contains N_g pairs. For the differentiated within-group and across-group relevances into the Group-based REC model training, the cross-modal relevance $R_{i,j}^{(g)}$ of any unmatched region-expression pair $\langle v_i^{(g)}, s_j^{(g)} \rangle$ ($i \neq j$, v_i or s_j is target) need to be embedded into Eq. 1 in an adaptive learning schema, where the pair $\langle v_{i'}^{(g)}, s_{j'}^{(g)} \rangle$ with the temporarily low relevance should be prior to the pair $\langle v_{i''}^{(g)}, s_{j''}^{(g)} \rangle$ with the temporarily high relevance. And the priority bias among $\{\langle v_i^{(g)}, s_j^{(g)} \rangle | v_i^{(g)}, s_j^{(g)} \in \mathcal{G}_g\}_{g=1}^{N_G}$ should be balanced over $\{\mathcal{G}_g | g = 1, \dots, N_G\}$.

B. Adaptive Priority Assignment

In the group of region-expression pairs, the cross-modal relevances are estimated/updated to assign the priorities to the unmatched pairs in different training iteration, which involves three key issues: (1) constructing the groups and pairs in advance, (2) extracting the textual and visual semantic features, and (3) estimating the cross-modal relevance and assigning the priority to the pair. We itemize them as follows:

Group and Pair Constructions. Given the region proposals $\{v_i | i \in 1, \dots, N\}$ and expressions $\{s_i | i \in 1, \dots, N\}$, we split them into N_G groups according to the subjectival categories of

⁴The pair set also contains the region/expression by default.

the expressions. In particular, according to the category list in the REC datasets, the categories of pairs, *e.g.*, *Person* category, are recognized by parsing the expressions via Stanford Parser [38] and locating the subject via pos-tag tool in NTLK [39]. Thus, we obtain the region proposals and expressions in groups, *i.e.*, $\{v_i^{(g)}, s_i^{(g)} | v_i^{(g)}, s_i^{(g)} \in \mathcal{G}_g\}_{g=1}^{N_g}$. Suppose there is a matched pair set \mathcal{P} with M randomly-sampled matched pairs in a certain batch, we re-index the pairs and formulate \mathcal{P} as $\{< v_i^{(g)}, s_i^{(g)} > | i = 1, \dots, M \text{ and } v_i^{(g)}, s_i^{(g)} \in \mathcal{G}_g\}_{g=1}^{N_g}$. Taking each region/expression in \mathcal{P} as the target, we construct the unmatched pair set by randomly sampling the negative expression/region s_j/v_k from the same group as the target. And the unmatched pair sets can be represented as $\mathcal{P}'_1 = \{< v_i^{(g)}, s_j^{(g)} > | v_i^{(g)} \in \mathcal{P}, s_j^{(g)} \in \text{Rand}(\mathcal{G}_g)\}_{g=1}^{N_g}$ and $\mathcal{P}'_2 = \{< v_k^{(g)}, s_i^{(g)} > | v_k^{(g)} \in \text{Rand}(\mathcal{G}_g), s_i^{(g)} \in \mathcal{P}\}_{g=1}^{N_g}$, where the number of the negatives is denoted as M' and j (or k) can be equal to i but with different meanings (negative vs. target). To reduce the inoperative correlations of objects and expressions in the pairs, we filter the pairs $< v_i, s_j >$ and $< v_j, s_i >$ according to the relative distance of v_i and v_j : if v_i and v_j are in the same image and their intersection-over-union (IoU) is less than 0.5, the corresponding pairs will be filtered out, otherwise kept. This helps to capture the spatial difference in each pair and prevent to construct the pairs with the redundant information of the same object.

Semantic Feature Extraction. To extract the semantic features of v and s (the superscript and the subscript are omitted for simplicity), we adopt the modular design [2] as our backbone due to its capability on handling different types of visual and textual semantic information. Specially, a Faster-RCNN based visual and a Bi-LSTM based textual modular attention networks are used to extract the semantic features of subjects, locations, and relationships in the images and the expressions, respectively. Note that, this part is not our innovation but it's indispensable for the subsequent relevance estimation.

For the textual semantic feature, given an expression $s = \{w_t\}_{t=1}^T$ with T words, we use a bi-directional LSTM (Bi-LSTM) [40] to encode the context for each word. In particular, word w_t is first embedded into a vector $\mathbf{e}_t \in R^d$ via word embedding. Then the Bi-LSTM is applied to encoding the whole expression upon $\{\mathbf{e}_t\}_{t=1}^T$ as:

$$\overrightarrow{\mathbf{h}}_t, \overleftarrow{\mathbf{h}}_t = \text{Bi-LSTM}(\mathbf{e}_t, \overrightarrow{\mathbf{h}}_{t-1}, \overleftarrow{\mathbf{h}}_{t+1}), \quad (2)$$

$$\mathbf{h}_t = \mathbf{W}_h [\overrightarrow{\mathbf{h}}_t, \overleftarrow{\mathbf{h}}_t], \quad (3)$$

where $\mathbf{W}_h \in R^{d \times 2d}$ is a weight matrix and $\mathbf{h}_t \in R^d$ is the t -th hidden feature derived from two directional LSTMs. $[\cdot, \cdot]$ is a concatenation operation. Finally, we compute the attention weights $\{a_t^m | m \in \{\text{subj}, \text{loc}, \text{rel}\}\}_{t=1}^T$ of the words for the three semantic items, *i.e.*, subject, location and relationship. The weighted sum of word embedding is made to represent three semantic items. These can be formulated as:

$$a_t^m = \frac{\exp(\mathbf{w}_m^T \mathbf{h}_t)}{\sum_{k=1}^T \exp(\mathbf{w}_m^T \mathbf{h}_k)}, \quad \mathbf{s}^m = \sum_{t=1}^T a_t^m \mathbf{e}_t, \quad (4)$$

where $\mathbf{w}_m \in R^d$ denotes the trainable vector over all expressions for each semantic item. $\mathbf{s}^{\text{subj}} \in R^d$, $\mathbf{s}^{\text{loc}} \in R^d$ and

$\mathbf{s}^{\text{rel}} \in R^d$ are subsequently concatenated into a feature vector $\mathbf{s} = [\mathbf{s}^{\text{subj}}, \mathbf{s}^{\text{loc}}, \mathbf{s}^{\text{rel}}]$ for the expression s .

For the visual semantic feature, we combine the three semantic items of region features upon Faster-RCNN. For the subject, we first extract the featuremaps $\mathbf{V} \in R^{c \times B}$ from the 4-th convolutional layers of ResNet [41] with grid size $B = 7 \times 7$ and channel c . Then, the attention of subject on the grid can be computed via:

$$\mathbf{H}_a = \tanh(\mathbf{W}_v \mathbf{V} + \mathbf{W}_s \mathbf{S}^{\text{subj}}), \quad \mathbf{H}_a \in R^{c' \times B}, \quad (5)$$

$$\mathbf{A} = \text{softmax}(\mathbf{w}_a^T \mathbf{H}_a), \quad \mathbf{A} \in R^B, \quad (6)$$

where $\mathbf{S}^{\text{subj}} \in R^{d \times B}$ is obtained by expanding \mathbf{s}^{subj} over B . $\mathbf{W}_v \in R^{d \times c}$, $\mathbf{W}_s \in R^{d \times d}$, and $\mathbf{w}_a \in R^d$ are the parameters of the non-linear mappings. Finally, the visual subject feature can be computed by the weighting sum of V , *i.e.*, $\mathbf{v}^{\text{subj}} = \sum_{i=1}^B \mathbf{A}_i \mathbf{V}_{\cdot, i}$.

For the location, we use a 5-dim vector \mathbf{l} to encode the top-left position (x_{tl}, y_{tl}) , the bottom-right position (x_{br}, y_{br}) , and the relative area of the region size $w \times h$ on the image size $W \times H$, *i.e.*, $\mathbf{l} = [\frac{x_{tl}}{W}, \frac{y_{tl}}{H}, \frac{x_{br}}{W}, \frac{y_{br}}{H}, \frac{w \cdot h}{W \cdot H}]$. Additionally, the relative location between the candidate region and each of its five surrounding regions (with the same category) is computed by using their position offsets and area ratio, *i.e.*, $\delta \mathbf{l}_j = [\frac{\Delta x_{tl,j}}{w}, \frac{\Delta y_{tl,j}}{h}, \frac{\Delta x_{br,j}}{w}, \frac{\Delta y_{br,j}}{h}, \frac{w_j \cdot h_j}{w \cdot h}]$ (the j -th surrounding region). $\{\delta \mathbf{l}_j\}_{j=1}^5$ is then concatenated into $\delta \mathbf{l}$. The final visual location feature can be computed as $\mathbf{v}^{\text{loc}} = \mathbf{W}_l[\mathbf{l}; \delta \mathbf{l}] + \mathbf{b}_l$.

For the relationship, we first find five arbitrary surrounding regions $\{v_j\}_{j=1}^5$ of the current candidate region, where their features of the final fully-connected layer are taken as the context features $\{\mathbf{v}_j^{\text{cxt}}\}_{j=1}^5$, and each of their position offsets to the current region is computed by $\delta \mathbf{l}'_j = [\frac{\Delta x_{tl,j}}{w}, \frac{\Delta y_{tl,j}}{h}, \frac{\Delta x_{br,j}}{w}, \frac{\Delta y_{br,j}}{h}, \frac{w_j \cdot h_j}{w \cdot h}]$. The final visual relationship feature is computed via $\hat{\mathbf{v}}_j^{\text{rel}} = \mathbf{W}_r[\mathbf{v}_j^{\text{cxt}}; \delta \mathbf{l}'_j] + \mathbf{b}_r$ and $\mathbf{v}_i^{\text{rel}} = [\{\hat{\mathbf{v}}_j^{\text{rel}}\}_{j=1}^5]$. The visual features of the above three items are finally concatenated as $\mathbf{v} = [\mathbf{v}^{\text{subj}}; \mathbf{v}^{\text{loc}}; \mathbf{v}^{\text{rel}}]$.

Cross-modal Relevance Estimation. The relevances of the unmatched region-expression pairs are estimated upon the above visual and textual semantic features of the pairs. For the unmatched pairs $< v_i^{(g)}, s_j^{(g)} >$ and $< v_k^{(g)}, s_i^{(g)} >$, $s_j^{(g)}$ and $v_k^{(g)}$ refer/belong to different objects and their corresponding region proposal $v_j^{(g)}$ or expression $s_k^{(g)}$ tend to be missing in the dataset.⁵ To this end, we estimate the cross-modal relevance by alternatively choosing the visual features or the textual features:

$$\mathbf{R}_{i,j}^{(g)} = \alpha \frac{[\mathbf{v}_i^{(g)}]^T \mathbf{v}_j^{(g)}}{\sum_{i',j'}^{M,M'} [\mathbf{v}_{i'}^{(g)}]^T \mathbf{v}_{j'}^{(g)}} + (1 - \alpha) \frac{[\mathbf{s}_i^{(g)}]^T \mathbf{s}_j^{(g)}}{\sum_{i',j'}^{M,M'} [\mathbf{s}_{i'}^{(g)}]^T \mathbf{s}_{j'}^{(g)}}, \quad (7)$$

where $\mathbf{R}^{(g)} \in R^{M \times M'}$ is a target-negative relevance matrix of the g -th group \mathcal{G}_g . $\mathbf{R}_{i,j}^{(g)}$ denotes the relevance between the i -th region/expression of the target and the j -th expression/region of the negative in the pair $< v_i^{(g)}, r_j^{(g)} >$ of \mathcal{G}_g . For simplicity, j can be equal to i but with different meanings as aforementioned. For $v_i^{(g)} \notin \mathcal{G}_g$ or $s_i^{(g)} \notin \mathcal{G}_g$, we set $\mathbf{R}_{i,j}^{(g)} = \text{Inf}$, which keeps the pairs of other groups out for the priority

⁵For example, the detected region proposals are probably not consistent with the existing regions with expressions.

assignment in \mathcal{G}_g . $\alpha \in \{0, 1\}$ is a switch coefficient to choose the visual or textual features for the relevance estimation. To assign the priorities to the unmatched pairs for training, we design an adaptive threshold to assign the binary value to the pair $\langle v_i^{(g)}, r_j^{(g)} \rangle$ according to its $\mathbf{R}_{i,j}^{(g)}$:

$$\mathbf{U}_{i,j}^{(g)} = \begin{cases} 1, \alpha = 1 \text{ and } \mathbf{R}_{i,j}^{(g)} < \lambda_1 + \tau\gamma, \\ 1, \alpha = 0 \text{ and } \mathbf{R}_{i,j}^{(g)} < \lambda_2 + \tau\gamma, \\ 0, \text{otherwise,} \end{cases} \quad (8)$$

where $\mathbf{U}^{(g)} \in R^{M \times M'}$ is a binary priority matrix of \mathcal{G}_g . The pair $\langle v_i^{(g)}, r_j^{(g)} \rangle$ is selected for the training if $\mathbf{U}_{i,j}^{(g)} = 1$, otherwise is discarded in the current iteration. In the right-hand side of the equation, λ_1 and λ_2 are the adaptive parameters to control the learning pace, where the number of the pairs with low relevances is dynamically decided. That is, the low-relevance pairs are preferentially used in the initial stage of the training and the higher-relevance pairs are gradually utilized with the model training. τ is a fixed trade-off coefficient and γ is the dynamically-changing coefficient (for the across-group relevance regularization term, detailed in Eq. 11 subsequently), which keep more various pairs utilized with the across-group relevance balanced, λ_1 , λ_2 and γ are updated as below:

$$\lambda_* \leftarrow \lambda_* + \frac{\mu_*}{M \cdot M'} \sum_{g=1}^{N_G} \sum_{i=1}^M \sum_{j=1}^{M'} \max(0, 1 - \mathbf{R}_{i,j}^{(g)}), \quad (9)$$

$$\gamma \leftarrow \eta\gamma, \quad (10)$$

where λ_* (λ_1 or λ_2) in the left side of the arrow is the updated parameter while the one in the right side is the previous value. λ_* is updated with the updating coefficient μ_* (μ_1 or μ_2) and the mean value of the counter-relevance matrices. This allows the model to adjust the stride of the learning pace: (1) when the regions and the expressions of the selected pairs averagely remain lowly relevant, the training will be easier (*e.g.*, significant differences of the appearance), and the model is able to learn from more various relevances. (2) with the relevances averagely increasing, there exist more various relevances to digest and the model begins to slow the learning stride down. For γ , it rises with the rate η during training. To prevent λ_* and γ from rising out of control, we set a upper limit for them as 1.

C. RMSL Objective

The proposed RMSL aims to embed differentiated within-group and across-group cross-modal relevances in an adaptive learning schema for Group-based REC. The main ideas of RMSL lie in two aspects: (1) the model should be trained by using lowly relevant unmatched pairs, prior to using highly relevant ones within each group, which can be regarded as learning a coarse-to-fine pattern step-by-step. (2) the relevances of the unmatched pairs from different groups should be balanced when these pairs are utilized in each training iteration. For the first idea, we design a specific learning schema, *i.e.*, *Relevance-guided SPL*, which uses the relevance updated in Section III-B to guided the self-paced learning. For

Algorithm 1: Training RMSL for Group-based REC

Input: The matched pair sets in $\{\mathcal{G}_g\}_{g=1}^{N_G}$
Output: The parameter set θ^*

- 1 Initialize the parameters θ , λ_1 , λ_2 and γ ; // Details are given in Section IV-A.
- 2 Initialize \mathcal{U} as Eq. 8;
- 3 **while** not converged **do**
 - // Pair Construction
 - 4 Construct \mathcal{P} from $\{\mathcal{G}_g\}_{g=1}^{N_G}$ by randomly sampling;
 - 5 Initialize \mathcal{P}'_1 , $\mathcal{P}'_2 = \emptyset$;
 - 6 **for** $i := 1$ to M **do**
 - 7 $\mathcal{P}'_1 = \mathcal{P}'_1 \cup \{\langle v_i^{(g)}, s_j^{(g)} \rangle | s_j^{(g)} \in \text{Rand}(\mathcal{G}_g)\}_{g=1}^{N_G};$
 - 8 $\mathcal{P}'_2 = \mathcal{P}'_2 \cup \{\langle v_k^{(g)}, s_i^{(g)} \rangle | v_k^{(g)} \in \text{Rand}(\mathcal{G}_g)\}_{g=1}^{N_G};$
 - 9 **end**
 - // Updating θ and \mathcal{U} .
 - 10 Update $\theta^* = \arg \min_{\theta} E(\mathcal{U}^*, \theta; \lambda, \gamma, \mathcal{P}, \mathcal{P}'_1, \mathcal{P}'_2)$;
// By the gradient-based method.
 - 11 Update $\mathcal{U}^* = \arg \min_{\mathcal{U}} E(\mathcal{U}, \theta^*; \lambda, \gamma, \mathcal{P}, \mathcal{P}'_1, \mathcal{P}'_2)$ as:
 - (1) Compute $\{\mathbf{R}^{(g)}\}_{g=1}^{N_G}$ as Eq. 7; // The visual and the textual semantic features can be updated using θ^* .
 - (2) Update \mathcal{U} as Eq. 8;
// Updating The Adaptive Parameters
 - 14 Update λ_1 and λ_2 as Eq. 9;
 - 15 Update γ as Eq. 10;
 - 16 **end**

the second ideas, we use a regularization term of the across-group relevance to reduce the group-wise relevance sparsity.

Relevance-guided SPL. In Group-based REC, the cross-modal relevances of the unmatched region-expression pairs are differentiated within each group, which leads to different effects of the pairs at different stages of model training. To embed the within-group cross-modal relevance into model training, we have updated the relevances based on the semantic features of the pairs and assigned their priorities to the pairs in the previous subsection. As a result, we obtain the priority matrices $\{\mathbf{U}^{(g)}\}_{g=1}^{N_G}$ (we use \mathcal{U} to represent the set/combination of these matrices), which indicate whether the pairs are selected according to the relevances. Following this, we minimize a relevance-masked triplet hinge loss in an adaptive manner:

$$E = \sum_{p_{i,i}^{(g)}, p_{i,j}^{(g)}, p_{k,i}^{(g)}} [\mathbf{U}_{i,j}^{(g)} Q(p_{i,i}^{(g)}, p_{i,j}^{(g)}; \theta) + \mathbf{U}_{i,k}^{(g)} Q(p_{i,i}^{(g)}, p_{k,i}^{(g)}; \theta)] - \frac{\lambda_1 + \lambda_2}{2} \|\mathcal{U}\|_1, \text{s.t. } p_{i,i}^{(g)} \in \mathcal{P}, p_{i,j}^{(g)} \in \mathcal{P}'_1, p_{k,i}^{(g)} \in \mathcal{P}'_2, \quad (11)$$

where $p_{i,i}^{(g)}$, $p_{i,j}^{(g)}$, and $p_{k,i}^{(g)}$ denote the pairs $\langle v_i^{(g)}, s_i^{(g)} \rangle$, $\langle v_i^{(g)}, s_j^{(g)} \rangle$, and $\langle v_k^{(g)}, s_i^{(g)} \rangle$, respectively. $Q(p_{i,i}^{(g)}, p_{i,j}^{(g)}; \theta)$ and $Q(p_{i,i}^{(g)}, p_{k,i}^{(g)}; \theta)$ are two max-margin functions formulated as below:

$$\begin{cases} \max(0, \Delta + F(v_i^{(g)}, s_j^{(g)}; \theta) - F(v_i^{(g)}, s_i^{(g)}; \theta)), \\ \max(0, \Delta + F(v_k^{(g)}, s_i^{(g)}; \theta) - F(v_i^{(g)}, s_i^{(g)}; \theta)), \end{cases} \quad (12)$$

where θ denotes the parameter set of the model that needs to be learned. Δ is the margin of the hinge loss. We mask the hinge loss in the top row of Eq. 11 with the binary priority matrix $\mathbf{U}^{(g)}$, which enables the model to selectively learn from different discriminations between the targets and the negatives in different stages. $\mathbf{U}^{(g)}$ is controlled by the adaptive parameters λ_1 and λ_2 in Eq. 8 and updated in each iteration via Eq. 9. This allows the pairs with high relevances are sequentially counted in the hinge loss with λ_* growing. In Eq. 11, $\frac{\lambda_1+\lambda_2}{2}\|\mathbf{U}\|_1$ is a regularizer, and the l_1 -norm can be written as:

$$\|\mathbf{U}\|_1 = \sum_{g=1}^{N_G} \sum_{i=1}^M \sum_{j=1}^{M'} \mathbf{U}_{i,j}^{(g)}. \quad (13)$$

where the l_1 -norm represents the number of the sampled pairs with the expected region-expression relevances (lower than λ_*), and the regularizer reflects the overall counter-relevance of the targets and the negatives. With Eq. 11 minimized, the regularizer is expected to be larger, which means the cross-modal relevances of the selected unmatched pairs are expected to be lower. This leads the model to focus on discriminating the wrong but ambiguous region-expression pairs.

Objective with Across-group Relevance Regularization. Since the relevance variance exists across different groups, this leads to the priority bias during the priority assignment of pairs. To reduce the bias and to balance the model training, we regularize the priority matrix set \mathbf{U} in a $l_{F,1}$ -norm term, formulated as:

$$\|\mathbf{U}\|_{F,1} = \sum_{g=1}^{N_G} \|\mathbf{U}^{(g)}\|_F, \quad (14)$$

where $\|\mathbf{U}^{(g)}\|_F$ is a Frobenius norm of $\mathbf{U}^{(g)}$. As indicated in [42], the $l_{2,1}$ -norm leads to a group-wise sparse representation of a vector if minimized. Inspired by this, we constrain \mathbf{U} in a $l_{F,1}$ -norm and maximize this term to make the counter-effect of group-wise sparsity, *i.e.*, non-zero items of $\{\mathbf{U}^{(g)}\}_{g=1}^{N_G}$ tend to be scattered across a large number of groups. In other words, the across-group relevance will be balanced and the variety of group will be ensured in this regularization. Integrated with this across-group relevance regularization, the total objective of RMSL can be rewritten as below:

$$\begin{aligned} E = & \sum_{\substack{p_{i,i}^{(g)}, p_{i,j}^{(g)}, p_{k,i}^{(g)} \\ p_{i,j}^{(g)}, p_{k,i}^{(g)}}} [\mathbf{U}_{i,j}^{(g)} Q(p_{i,i}^{(g)}, p_{i,j}^{(g)}; \theta) + \mathbf{U}_{i,k}^{(g)} Q(p_{i,i}^{(g)}, p_{k,i}^{(g)}; \theta)] \\ & - \frac{\lambda_1+\lambda_2}{2} \|\mathbf{U}\|_1 - \gamma \|\mathbf{U}\|_{F,1}, \\ \text{s.t. } & p_{i,i}^{(g)} \in \mathcal{P}, p_{i,j}^{(g)} \in \mathcal{P}'_1, p_{k,i}^{(g)} \in \mathcal{P}'_2, \end{aligned} \quad (15)$$

where γ is the dynamically-changing coefficient in the across-group relevance regularization. And it is updated as Eq. 10, which makes the model to increase the attention on the across-group relevance balancing when the model learns to distinguish the matched/unmatched pairs and estimate the region-expression relevances. For the model training, we minimize

$E(\mathbf{U}, \theta)$ in Eq. 15 to optimize the parameter set θ and the priority matrix set \mathbf{U} .

Optimization Strategy. The objective function in the traditional SPL is convex while the one in the proposed RMSL is non-convex due to the $l_{F,1}$ -norm of the priority matrix set \mathbf{U} . Consequently, the traditional gradient-based methods cannot be directly applied to the optimization of $\mathbf{U}^* = \arg \min_{\mathbf{U}} E(\mathbf{U}, \theta)$. To this end, we adopt an alternative convex search (ACS) algorithm [10], [43] for the biconvex optimization of RMSL. In particular, the parameter set θ and the priority matrix set \mathbf{U} are optimized in an alternative way as shown in Alg. 1. In each iteration, θ is first optimized by the gradient-based method while keeping \mathbf{U} fixed. And \mathbf{U} is then updated via Eq. 8 while keeping θ fixed. The self-paced parameters λ_1 , λ_2 , and γ are subsequently updated with strides μ_1 , μ_2 , and η according to Eq. 9 and Eq. 10, respectively.

IV. EXPERIMENTS

In this section, we first describe the experimental settings, including preprocessing, parameter settings, datasets, evaluation protocols, and competitive methods. Next, we quantitatively compare the results of our proposed model to the state-of-the-art methods on REC. Finally, we conduct detailed model analysis on the within-group and the across-group relevances respectively.

A. Experimental Settings

Training Settings. In this part, we provide the training settings on four aspects, including sample sizes, parameter settings, variable dimensions, and training details. For sample sizes, we set the target number M and the negative number M' in each batch as 10 and 60, where each target is paired with 6 negatives in $\mathcal{P}'_1, \mathcal{P}'_2$. For parameter settings, λ_1 , λ_2 , and γ are all initialized to 0.5 and updated once every 1,000 iterations. μ_1 , μ_2 , τ , and Δ are empirically set as 0.1. η is set as 1.1. The weights in θ are all initialized randomly in $[0, 1]$. For variable dimensions, the word embedding size and hidden state size of the LSTM are set to 512. The outputs of all MLPs and FCs in the model are also set to be 512-dimensional. For training details, we adopt Adam [47] as the gradient-based method, where the initial learning rate is set as $4e^{-4}$ and halved every 8,000 iterations after the first 8,000-iteration warm-up. To avoid overfitting, we regularize the word-embedding and output layers of the LSTM in the textual attention network using dropout with ratio of 0.5. The method is implemented in PyTorch, which takes roughly 57 training hours on NVIDIA GTX 1080 Ti GPU.

Datasets. We evaluate on three widely-used datasets for REC, *i.e.*, RefCOCO [4], RefCOCO+ [4], and RefCOCOg [3], all of which are collected from the MSCOCO dataset [48].

RefCOCO (UNC RefExp) contains 142,209 referring expressions for 50,000 objects in 19,994 images from COCO. Since *Person* is much more frequent than other objects in the dataset, the split is person vs. objects: images containing multiple persons are in “Test A” and images containing multiple objects from other categories are in “Test B”.

TABLE II

PERFORMANCE COMPARISONS AGAINST THE STATE-OF-THE-ART METHODS ON GROUND-TRUTH REGIONS. ALL VALUES ARE IN %. THE BEST RESULTS ARE MARKED IN **BOLD**

	RefCOCO			RefCOCO+			RefCOCOg		
	val	testA	testB	val	testA	testB	val*	val	test
MMI [3]	-	63.15	64.21	-	48.73	42.13	62.14	-	-
NegBag [18]	76.90	75.60	78.00	-	-	-	-	-	68.40
visdif+MMI [4]	-	73.98	76.59	-	59.17	55.62	64.02	-	-
Luo [15]	-	74.04	73.43	-	60.26	55.03	65.36	-	-
CMN [1]	-	-	-	-	-	-	69.30	-	-
Speaker/visdif [4]	76.18	74.39	77.30	58.94	61.29	56.24	59.40	-	-
S-L-R [16]	79.56	78.95	80.22	62.26	64.60	59.62	72.63	71.65	71.92
Attr [5]	-	78.05	78.07	-	61.47	57.22	69.83	-	-
VC [44]	-	78.98	82.39	-	62.56	62.90	73.98	-	-
A-ATT [45]	81.27	81.17	80.01	65.56	68.76	60.63	73.18	-	-
PLAN [17]	81.67	80.81	81.32	64.18	66.31	61.46	69.47	-	-
Multi-hop FiLM [46]	84.9	87.4	83.1	73.8	78.7	65.8	71.5	-	-
MAttN [2]	83.85	85.42	83.18	71.31	74.22	66.24	-	77.27	76.82
RMSL-WG	84.79	86.61	83.15	71.58	73.20	66.18	-	78.47	77.63
RMSL-AG	84.63	85.88	82.95	71.44	73.15	66.25	-	78.37	77.43
RMSL	85.92	87.50	83.67	72.10	73.95	66.47	-	79.15	78.42

TABLE III

PERFORMANCE COMPARISONS IN THE GROUP-BASED SCHEME ON REFCOCOG. ALL VALUES ARE IN %

	val	Inc.	test	Inc.
MAttN	77.27	-	76.82	-
MAttN-g	77.45	+0.18	77.05	+0.23
RMSL	79.15	+1.88	78.42	+1.60

RefCOCO+ has 141,564 expressions for 49,856 objects in 19,992 images from COCO, which is also collected using ReferitGame. Different from RefCOCO dataset, players (annotators) are not allowed to use location words to describe objects. Therefore, this dataset focuses more on the pure appearance based description. The split in RefCOCO+ follows the same rule used in RefCOCO.

RefCOCOg (*Google RefExp*) consists of 85,474 referring expressions for 54,822 objects in 26,711 images from COCO. Different from RefCOCO and RefCOCO+, this dataset is collected using a non-interactive setting and contains much longer sentences. The dataset is randomly partitioned into training, validation (“val”) and testing (“test”) splits.

Evaluation Protocols. For evaluation, we adopt two commonly-used settings in REC [2], [5], [16]. In the first setting, ground-truth bounding boxes are taken as the candidate regions, and a localization is correct if the best-matching region is consistent with the ground-truth. In the second setting, the candidate regions are extracted by the object detection model, and a localization is correct if the intersection-over-union (IoU) of the best-matching region with the ground-truth bounding box is greater than 0.5. Since REC focuses on visual-textual correspondence and comprehension of cross-modal information, rather than detection performance, we report results under both settings, and conduct analysis and ablation study with the first setting, where the metric is called accuracy (ACC).

Competitive Methods. We compare the proposed RMSL schema with six baselines: (1) MAttN (state-of-the-art): A joint embedding model to match the region and expression in each image by using multiple modular attention networks

[2] (reproduced by using the official code⁶). (2) MAttN-g: An alternative version of MAttN by randomly selecting pairs in the group-based scheme. (3) RandSel-WG: An alternative version of RMSL, where the sample pairs are randomly selected from each group uniformly to validate the significance of the differentiated within-group relevance. (4) RandSel-AG: An alternative version of RMSL, where the sample pairs are selected upon their pairwise relevance but randomly from different groups to validate the significance of the differentiated across-group relevance. (5) RMSL-WG: An alternative version of RMSL without the balance constraint of the across-group relevance (without the across-group relevance regularization term). (6) RMSL-AG: An alternative version of RMSL without within-group relevance regularization term. Other competitive methods include MMI [3], NegBag [18], visdif+MMI [4], Luo [15], CMN [1], Speaker/visdif [4], S-L-R [16], Attr [5], PLAN [17], and Multi-hop FiLM [46].

B. Comparison to the State-of-the-art

There are two experimental settings for the comprehension task. The first setting assumes that the observer has already known what an object is, so the input region set consists of all the ground truth candidates labeled in the MSCOCO dataset. The model is required to select the target object from those ground truth objects. The second setting assumes that the whole process is conducted automatically. The model needs to detect potential objects (we use Faster-RCNN [13] as the detector in this paper) from the image in the first place.

We first compare the proposed RMSL model with state-of-the-art methods using MSCOCO’s ground-truth bounding boxes as object proposals. Results of the comparisons on RefCOCO, RefCOCO+, and RefCOCOg datasets are shown in Tab. II. The proposed RMSL achieves the best performance on most evaluation sets, which demonstrates the superiority and effectiveness of the proposed learning scheme. In Tab. II, RMSL outperforms MAttN on most metrics, specially, around 2% on the RefCOCOg dataset, which reflects that considering

⁶<https://github.com/lichengunc/MAttNet>

TABLE IV
PERFORMANCE COMPARISONS AGAINST THE STATE-OF-THE-ART METHODS ON THE FULLY-AUTOMATIC COMPREHENSION TASK. ALL VALUES ARE IN %.
THE BEST RESULTS ARE MARKED IN **BOLD**

	RefCOCO			RefCOCO+			RefCOCOg	
	val	testA	testB	val	testA	testB	val	test
Luo [15]	-	67.94	55.18	-	57.05	43.33	-	-
S-L-R [16]	69.48	73.71	64.96	55.71	60.74	48.80	60.21	59.63
PLAN [17]	-	75.31	65.52	-	61.34	50.86	-	-
MAttN [2]	75.82	80.75	69.58	65.41	70.35	56.12	66.85	66.66
RMSL-WG	76.44	80.23	69.51	65.67	70.78	56.29	66.97	66.47
RMSL-AG	76.83	80.50	69.64	65.89	70.45	56.50	67.12	67.03
RMSL	77.60	81.08	70.12	66.22	71.14	57.86	67.99	67.67

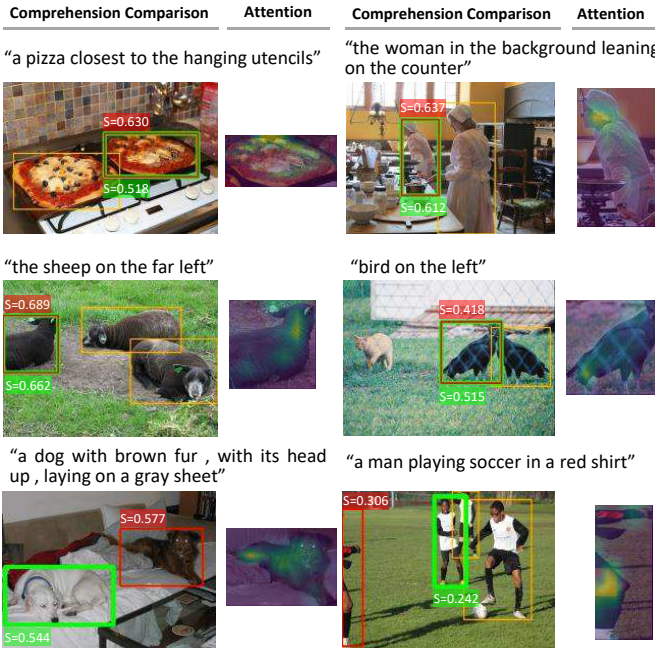


Fig. 3. Visualized examples of REC. The red and green boxes (with matching scores) are the localization results of the proposed RMSL and MAttN, respectively. The orange boxes are presented for the region candidates.

the differentiated within-group and across-group relevances does contribute to the semantic comprehension of regions and expressions. We also compare RMSL to the alternative versions of RMSL without the constraints of the within-group relevance (RMSL-AG) or the across-group relevance (RMSL-WG) in Tab. II, where RMSL outperforms RMSL-WG and RMSL-AG. This confirms the merits of integrating within-group and across-group relevances in the task of Group-based REC. The effectiveness of modeling differentiated relevances is also verified in Tab. III, where the increase of RMSL exceeds MAttN-g in the case of group-based scheme. This also reflects the low effect of group data on the performance improvement, which is probably due to many inoperative pairs.

Utilizing automatically detected objects enables an in-depth analysis of fully automatic comprehension performance for REC task. We then show the comparison results with the state-of-the-arts using automatically detected objects from Faster-RCNN in Tab. IV. The overall performance drops (compared to Tab. II) due to detection errors. Additionally, the proposed RMSL keeps the best performance on all the evaluation

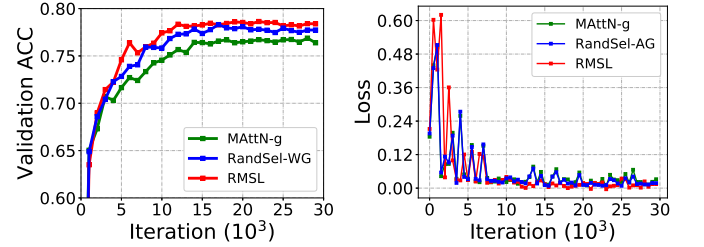


Fig. 4. Training curves of the proposed RMSL, RandSel-WG, and MAttN-g on the same grouped data. Curves of validation ACC are shown in the right side, and the left is for the curves on training loss.

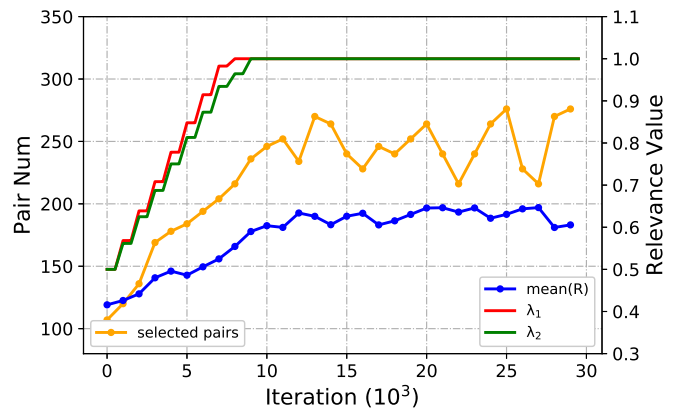


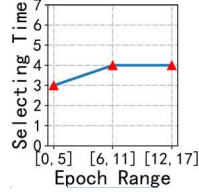
Fig. 5. Changing curves of selected pair number (per batch), average batch relevance “mean(R)”, parameters λ_1 and λ_2 at different iterations. “Relevance Value” is the general relevance-related score for “mean(R)”, λ_1 and λ_2 .

sets, which reflected the robustness of the learning scheme on different sources of data. Specially, RMSL outperforms MAttN on RefCOCOg dataset, where much longer expressions/sentences are contained in this dataset. It reflects that longer expressions/sentences can also be embedded effectively during relevance estimation.

Finally, we show some visualized examples by employing both the proposed RMSL and MAttN in Fig. 3. In the top two rows, both two methods can locate the correct regions. However, with respect to some complex pairs in the bottom row, *e.g.*, long expression (the right-bottom case) and missing parts (the left-bottom case), RMSL achieves better comprehension, due to the distinction of diverse pairs during the model training.

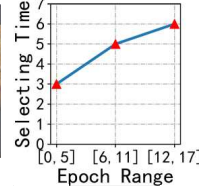
Targ: a silver laptop to the left of a desktop monitor

Neg: laptop closest to camera



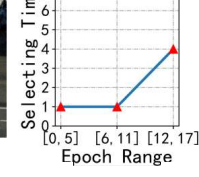
Targ: the pizza that is by the fork

Neg: uncut portion of a large pizza



Targ: bike on right

Neg: the motor cycle visible between the other two and running behind



Targ: the two giraffes to the left of one giraffe

Neg: a giraffe to the left of another giraffe

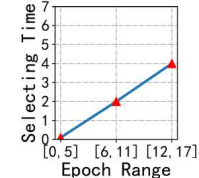


Fig. 6. Examples of the unmatched target (Red)-negative (Blue) pairs with the highest (Top) and the lowest (Bottom) diversities. The curves show the selecting times of the corresponding pairs during several epoches.

C. Ablation on Within-group Relevance

The effect of the within-group relevance can be analyzed from three aspects, *i.e.*, training curves, change of data during data selection, and different examples with different relevances. Specially, we first present the training curves of different methods in each iteration in Fig. 4. Clearly, the performance of RMSL increases faster than RandSel-WG at the beginning, which shows the effectiveness of embedding the differentiated within-group relevance in the pair selection. Additionally, RMSL reaches the best value among the three methods on the validation accuracy after around 2,500 iterations, which verifies the superiority of the relevance-guided data selection and training scheme. Although the loss curve of RMSL fluctuates obviously in the early stage, it converges better after around 7,500 iterations, which may stem from the better selection on the training samples and better feature representation for different relevances.

Secondly, to analyze the process of the data selection, we present the changing curves on the number of unmatched pairs selected, the average batch relevance, and the parameters λ_1 and λ_2 at different iterations in Fig. 5. During the model training, more and more unmatched pairs are selected with the increase of parameters λ_1 and λ_2 , which reflects the stability and effectiveness on selecting the pairs with different relevance.

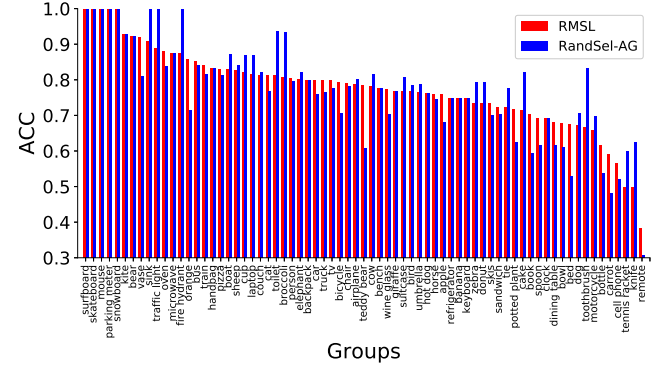


Fig. 7. Group-wise comparisons on ACC between the methods with and without considering the across-group relevance (RMSL vs. RandSel-AG).

TABLE V

THE EFFECT OF THE ACROSS-GROUP RELEVANCE REGULARIZATION (AG-R) ON THE PAIR SELECTION OVER DIFFERENT GROUPS. “M” DENOTES THE MEAN NUMBERS OF THE SELECTED PAIRS AMONG GROUPS IN DIFFERENT ITERATION RANGES (“ITER RANGE”, $\times 10^3$). HERE, “CV” (COEFFICIENT OF VARIATION [9]) DENOTES THE RATIO (%) OF THE STANDARD DEVIATION OF PAIR NUMBERS (OVER DIFFERENT GROUPS) TO THEIR MEAN NUMBER

Iter Range	(0,5]	(5,10]	(10,15]	(15,20]	(20,25]	(25,30]
w/o	M	12598	12835	12853	12857	12852
	CV	88.64	88.57	88.86	88.46	88.74
AG-R	M	13120	13377	13391	13393	13385
	CV	86.15	84.73	83.60	83.34	83.48

vances. Moreover, the average batch relevance grows gradually in the early stage of training and turns to level off, while the selected pair number grows observably in the early stage of training and turns to sharp fluctuation afterwards. These confirm that the pairs with low relevances are selected in the early stage of training and the pairs with high relevances are selected gradually, during which the number of the selected pairs doesn't always grow when λ_1 and λ_2 reach the maximums. Besides, Fig. 4 shows that RMSL outperforms the other two at the beginning, *e.g.*, at iteration 5×10^3 , while few pairs are selected (see the cyan curve in Fig. 5), which reflects that the (low) relevance of the data, rather than its scale or its variety, affects the performance. The pairs with higher relevances are gradually selected, which can be seen as an adaptive sampling process to overcome the overfitting. It further reveals the robustness and the adaptiveness of the proposed RMSL model on selecting complex samples.

Finally, we show the examples of the unmatched pairs with the lowest and highest relevances in Fig. 6. Comparing the visual and the textual contents, the relevances of the pairs between the top two and the bottom two rows vary greatly. For example, the two pizzas (in the second row) appear less relevant compared to the giraffe pairs (in the bottom row). It verifies the ability of capturing the relevance in the RMSL model. Moreover, as the curves show, the pairs with low relevances are selected more often in the beginning, while the pairs with high relevances are selected gradually up to the similar times as the formers, which further validates the effectiveness of our sample selection scheme.

D. Ablation on Across-group Relevance

We conduct four subdivided experiments to evaluate the role of across-group relevance in the proposed RMSL schema. Specially, we first compare the accuracies of different groups with and without the constraint of the across-group relevance in Fig. 7, from which we find that the performances of different groups are more balanced after considering the constraint of the across-group relevance during model training. It reflects the effectiveness of the constraint to reduce the bias of specific categories. Additionally, the red redundant area is apparently larger than the green one, which indicates the superiority of the proposed RMSL on the performances among most groups.

Then, we analyze the internal effect of the across-group relevance regularization $\|\mathcal{U}\|_{F,1}$ in Tab. V. Since across-group relevance regularization decides the priority balance of pairs, we can analyze it on the numbers of the selected pairs for different groups. Tab. V shows the mean number of the selected pairs among groups in different iteration ranges, as well as the ratio of the standard deviation of the pair numbers (over different groups) to their mean number. We can find that the mean numbers with across-group relevance regularization in different ranges are larger than the ones without the regularization, which reflects the counter-sparsity effect of the regularization on pair selection over groups. Besides, the “CV” with across-group relevance regularization in each range is lower than the ones without the regularization, which manifests the ability of the regularization on balancing the priorities of different groups. Moreover, with the iteration increasing, the “CV” with the regularization tends to flatten. This indicates the controllability of the across-group relevance balancing in the overall schema.

Next, we further analyze the average validation ACC of different groups at different iterations in Fig. 8. Whether RandSel-AG outperforms RMSL or not on the ACC of each group, the group ACC curves of RMSL tend to be close to its average ACC curves, which reflects the effect of the across-group relevance constraint on balancing the multi-group training. Additionally, from the average ACC curves, we find that RMSL is enhanced by the across-group relevance constraint, which surpasses RandSel-AG during almost the entire training period. This reflects the overall effect of the across-group relevance.

Finally, we compare the proposed RMSL with RandSel-AG on the average ACC (AVE) and the corresponding standard deviation (STD) over different groups in Tab. VI. We compute the AVEs and STDs at the 0.5K-th, 1K-th, 5K-th, and 10K-th iterations, respectively. Clearly, the AVEs of the proposed RMSL are higher than the ones of RandSel-AG, but with much smaller STDs. It demonstrates that the across-group relevance constraint not only boosts the overall learning performance, but also reduces the bias of certain categories.

V. CONCLUSION

In this paper, we propose a new but general problem about referring expression comprehension, *i.e.*, Group-based REC, where the cross-modal relevances of region-expression pairs are differentiated within each group and across different

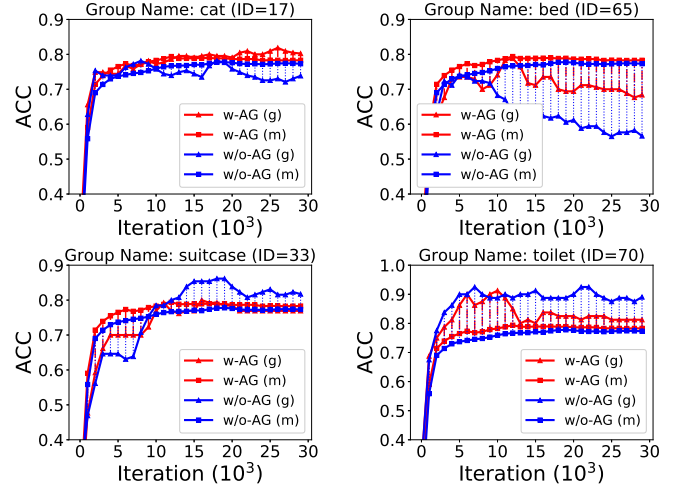


Fig. 8. Average validation ACC curves of some specific groups (curves with triangle markers) at different iterations (“(g)”). Curves with square markers are the average ACC of all the groups (“(m)”). The red and blue colors denote RMSL (“w-AG”) and RandSel-AG (“w/o-AG”) respectively. The top and the bottom examples are presented to show the higher performance of RMSL and RandSel-AG on the group ACC, respectively.

TABLE VI

COMPARISONS ON THE AVERAGE ACC (AVE) AND THE CORRESPONDING STANDARD DEVIATION (STD) OVER DIFFERENT GROUPS AT DIFFERENT TRAINING ITERATIONS. ALL VALUES ARE IN %

	Iter (0.5K)	Iter (1K)	Iter (5K)	Iter (10K)
AVE	RandSel-AG	60.07	65.75	74.05
	RMSL	62.45	66.56	75.30
STD	RandSel-AG	17.81	15.30	13.01
	RMSL	17.26	14.80	12.67

groups. To distinguish the visual/textual semantics, we further propose a novel relevance-guided multi-group self-paced learning schema (termed RMSL) to embed the within-group and across-group relevances into an adaptive learning cycle, where the within-group region-expression pairs are adaptively assigned with different priorities according to their cross-modal relevances, and the bias of the group priority is balanced via an across-group relevance constraint. The relevances, the pairs, and the model parameters are alternately updated during an end-to-end adaptive model training. We have demonstrated that the proposed RMSL schema achieves superior performance over the state-of-the-art REC methods [1], [2], [5], [15]–[17] on three widely-used benchmarks (RefCOCO, RefCOCO+, and RefCOCOg). We have also conducted extensive ablative experiments to further demonstrate the effectiveness of RMSL on modeling differentiated within-group and across-group relevances.

In the future, we would like to further investigate Group-based REC on the vertical and horizontal aspects: (1) Although it's natural for human to efficiently learn and comprehend the language-vision semantics from easily distinguished samples to hardly distinguished ones, some types of samples (*e.g.*, region-expression pairs in some groups) tend to be missing or appear in a few-shot case, making the learning difficult. It would be inspirational to advance the proposed adaptive learning strategy to consider the group-wise correlation of

the semantic attributes. (2) Some computer vision tasks like Person Re-identification [49], [50] can also be transformed into group-based problems by modeling the semantic relevances of the target and negative regions. It would be interesting and potential to explore the feasibility of the proposed adaptive learning strategy on these tasks.

ACKNOWLEDGMENT

This work is supported by the National Key R&D Program (No.2017YFC0113000, and No.2016YFB1001503), Nature Science Foundation of China (No.U1705262, No.61772443, and No.61572410), Post Doctoral Innovative Talent Support Program under Grant BX201600094, China Post-Doctoral Science Foundation under Grant 2017M612134, Scientific Research Project of National Language Committee of China (Grant No. YB135-49), and Nature Science Foundation of Fujian Province, China (No. 2017J01125 and No. 2018J01106).

REFERENCES

- R. Hu, M. Rohrbach, J. Andreas, T. Darrell, and K. Saenko, "Modeling relationships in referential expressions with compositional modular networks," in *CVPR*, 2017, pp. 4418–4427.
- L. Yu, Z. Lin, X. Shen, J. Yang, X. Lu, M. Bansal, and T. L. Berg, "Mattnet: Modular attention network for referring expression comprehension," in *CVPR*, 2018.
- J. Mao, J. Huang, A. Toshev, O. Camburu, A. L. Yuille, and K. Murphy, "Generation and comprehension of unambiguous object descriptions," in *CVPR*, 2016, pp. 11–20.
- L. Yu, P. Poirson, S. Yang, A. C. Berg, and T. L. Berg, "Modeling context in referring expressions," in *ECCV*, 2016, pp. 69–85.
- J. Liu, L. Wang, M.-H. Yang *et al.*, "Referring expression generation and comprehension via attributes," in *ICCV*, 2017.
- A. Prasad, S. Jegelka, and D. Batra, "Submodular meets structured: Finding diverse subsets in exponentially-large structured item sets," in *NeurIPS*, 2014, pp. 2645–2653.
- L. Jiang, D. Meng, S.-I. Yu, Z. Lan, S. Shan, and A. Hauptmann, "Self-paced learning with diversity," in *NeurIPS*, 2014, pp. 2078–2086.
- V. Kaushal, A. Sahoo, K. Doctor, N. Raju, S. Shetty, P. Singh, R. Iyer, and G. Ramakrishnan, "Learning from less data: Diversified subset selection and active learning in image classification tasks," *arXiv preprint arXiv:1805.11191*, 2018.
- H. Abdi, "Coefficient of variation," *Encyclopedia of research design*, vol. 1, pp. 169–171, 2010.
- M. P. Kumar, B. Packer, and D. Koller, "Self-paced learning for latent variable models," in *NIPS*, 2010, pp. 1189–1197.
- L. Jiang, D. Meng, T. Mitamura, and A. G. Hauptmann, "Easy samples first: Self-paced reranking for zero-example multimedia search," in *ACM MM*, 2014, pp. 547–556.
- Y. Ren, P. Zhao, Y. Sheng, D. Yao, and Z. Xu, "Robust softmax regression for multi-class classification with self-paced learning," in *AAAI*, 2017, pp. 2641–2647.
- S. Ren, K. He, R. Girshick, and J. Sun, "Faster r-cnn: Towards real-time object detection with region proposal networks," in *NIPS*, 2015, pp. 91–99.
- D. Bahdanau, K. Cho, and Y. Bengio, "Neural machine translation by jointly learning to align and translate," *arXiv preprint arXiv:1409.0473*, 2014.
- R. Luo and G. Shakhnarovich, "Comprehension-guided referring expressions," in *CVPR*, vol. 2, 2017.
- L. Yu, H. Tan, M. Bansal, and T. L. Berg, "A joint speaker-listener-reinforcer model for referring expressions," in *CVPR*, vol. 2, 2017.
- B. Zhuang, Q. Wu, C. Shen, I. Reid, and A. van den Hengel, "Parallel attention: A unified framework for visual object discovery through dialogs and queries," in *CVPR*, 2018, pp. 4252–4261.
- V. K. Nagaraja, V. I. Morariu, and L. S. Davis, "Modeling context between objects for referring expression understanding," in *ECCV*, 2016, pp. 792–807.
- R. Hu, H. Xu, M. Rohrbach, J. Feng, K. Saenko, and T. Darrell, "Natural language object retrieval," in *CVPR*, 2016, pp. 4555–4564.
- A. Rohrbach, M. Rohrbach, R. Hu, T. Darrell, and B. Schiele, "Grounding of textual phrases in images by reconstruction," in *ECCV*, 2016, pp. 817–834.
- K. Chen, R. Kovvuri, and R. Nevatia, "Query-guided regression network with context policy for phrase grounding," in *ICCV*, 2017.
- Y. Bengio, J. Louradour, R. Collobert, and J. Weston, "Curriculum learning," in *ICML*, 2009, pp. 41–48.
- A. Pentina, V. Sharmanska, and C. H. Lampert, "Curriculum learning of multiple tasks," in *CVPR*, 2015, pp. 5492–5500.
- Y. Shi, M. Larson, and C. M. Jonker, "Recurrent neural network language model adaptation with curriculum learning," *Computer Speech & Language*, vol. 33, no. 1, pp. 136–154, 2015.
- C. Gong, D. Tao, S. J. Maybank, W. Liu, G. Kang, and J. Yang, "Multi-modal curriculum learning for semi-supervised image classification," *IEEE Transactions on Image Processing*, vol. 25, no. 7, pp. 3249–3260, 2016.
- A. Graves, M. G. Bellemare, J. Menick, R. Munos, and K. Kavukcuoglu, "Automated curriculum learning for neural networks," in *ICML*, 2017, pp. 1311–1320.
- L. Jiang, D. Meng, Q. Zhao, S. Shan, and A. G. Hauptmann, "Self-paced curriculum learning," in *AAAI*, vol. 2, no. 5.4, 2015, p. 6.
- D. Meng, Q. Zhao, and L. Jiang, "A theoretical understanding of self-paced learning," *Information Sciences*, vol. 414, pp. 319–328, 2017.
- Y. Fan, R. He, J. Liang, and B.-G. Hu, "Self-paced learning: An implicit regularization perspective," in *AAAI*, vol. 3, 2017, p. 4.
- D. Zhang, D. Meng, C. Li, L. Jiang, Q. Zhao, and J. Han, "A self-paced multiple-instance learning framework for co-saliency detection," in *ICCV*, 2015, pp. 594–602.
- D. Zhang, D. Meng, and J. Han, "Co-saliency detection via a self-paced multiple-instance learning framework," *IEEE Transactions on Pattern Analysis and Machine Intelligence*, vol. 39, no. 5, pp. 865–878, 2017.
- D. Zhang, J. Han, L. Zhao, and D. Meng, "Leveraging prior-knowledge for weakly supervised object detection under a collaborative self-paced curriculum learning framework," *International Journal of Computer Vision*, pp. 1–18, 2018.
- S. Zhou, J. Wang, D. Meng, X. Xin, Y. Li, Y. Gong, and N. Zheng, "Deep self-paced learning for person re-identification," *Pattern Recognition*, vol. 76, pp. 739–751, 2018.
- D. Ouyang, J. Shao, Y. Zhang, Y. Yang, and H. T. Shen, "Video-based person re-identification via self-paced learning and deep reinforcement learning framework," in *ACM MM*, 2018, pp. 1562–1570.
- H. Li and M. Gong, "Self-paced convolutional neural networks," in *IJCAI*, 2017, pp. 2110–2116.
- L. Lin, K. Wang, D. Meng, W. Zuo, and L. Zhang, "Active self-paced learning for cost-effective and progressive face identification," *IEEE Transactions on Pattern Analysis and Machine Intelligence*, vol. 40, no. 1, pp. 7–19, 2018.
- L. Jiang, "Web-scale multimedia search for internet video content," in *WWW*, 2016, pp. 311–316.
- R. Socher, C. C. Lin, C. Manning, and A. Y. Ng, "Parsing natural scenes and natural language with recursive neural networks," in *Proceedings of the 28th international conference on machine learning (ICML-11)*, 2011, pp. 129–136.
- E. Loper and S. Bird, "Nltk: the natural language toolkit," *arXiv preprint cs/0205028*, 2002.
- A. Graves and J. Schmidhuber, "Framewise phoneme classification with bidirectional lstm and other neural network architectures," *Neural Networks*, vol. 18, no. 5–6, pp. 602–610, 2005.
- K. He, X. Zhang, S. Ren, and J. Sun, "Deep residual learning for image recognition," in *CVPR*, 2016, pp. 770–778.
- Y. Ming and L. Yi, "Model selection and estimation in regression with grouped variables," *Journal of the Royal Statistical Society*, vol. 68, no. 1, pp. 49–67, 2006.
- K. Tang, V. Ramanathan, L. Fei-Fei, and D. Koller, "Shifting weights: Adapting object detectors from image to video," in *NeurIPS*, 2012, pp. 638–646.
- H. Zhang, Y. Niu, and S.-F. Chang, "Grounding referring expressions in images by variational context," in *CVPR*, 2018, pp. 4158–4166.
- C. Deng, Q. Wu, Q. Wu, F. Hu, F. Lyu, and M. Tan, "Visual grounding via accumulated attention," in *CVPR*, 2018, pp. 7746–7755.
- F. Strub, M. Seurin, E. Perez, H. De Vries, J. Mary, P. Preux, and A. CourvilleOlivier Pietquin, "Visual reasoning with multi-hop feature modulation," in *ECCV*, 2018, pp. 784–800.
- D. P. Kingma and J. Ba, "Adam: A method for stochastic optimization," *arXiv preprint arXiv:1412.6980*, 2014.

- [48] T.-Y. Lin, M. Maire, S. Belongie, J. Hays, P. Perona, D. Ramanan, P. Dollár, and C. L. Zitnick, "Microsoft coco: Common objects in context," in *ECCV*, 2014, pp. 740–755.
- [49] L. Zheng, L. Shen, L. Tian, S. Wang, J. Wang, and Q. Tian, "Scalable person re-identification: A benchmark," in *ICCV*, 2015, pp. 1116–1124.
- [50] W. Li, X. Zhu, and S. Gong, "Harmonious attention network for person re-identification," in *CVPR*, 2018, pp. 2285–2294.